

New Hybrid Controller Using Optimal Design of Coefficient Diagram Method (CDM) to Automatic Voltage Regulator (AVR) Through Turbulent Flow of Water-based Optimization Algorithm

Due Mina Heshmati¹, Iraj Faraji², Saeid Jalilzadeh^{1,*}, Reza Noroozian¹ and Hosein Shayeghi²

¹University of Zanjan, Iran

²University of Mohaghegh, Iran

*Corresponding Author: Saeid Jalilzadeh, University of Zanjan, Iran, E-mail: jalilzadeh@znu.ac.ir

Citation: Due Mina Heshmati, Iraj Faraji, Saeid Jalilzadeh, Reza Noroozian, Hosein Shayeghi (2024) New Hybrid Controller Using Optimal Design of Coefficient Diagram Method (CDM) to Automatic Voltage Regulator (AVR) Through Turbulent Flow of Water-based Optimization Algorithm. 1: 1-23

Received Date: November 05, 2024

Accepted Date: December 05, 2024

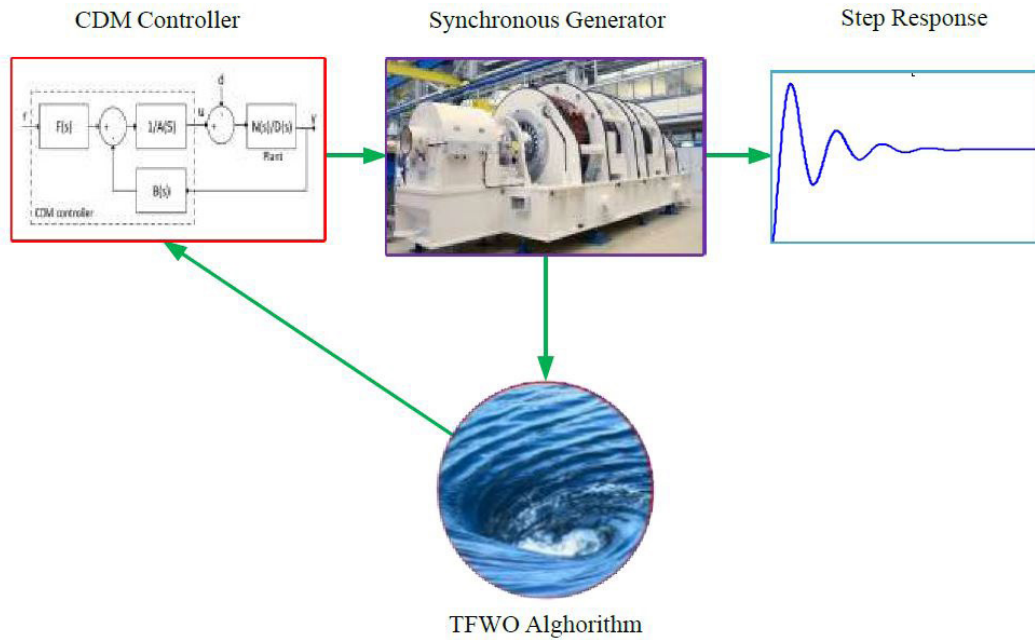
Published Date: December 08, 2024

Abstract

Changes in the power demand, such as changes in consumption patterns during the COVID-19 era, have caused voltage fluctuations in the power system. One of the most straightforward approach to controlling such fluctuations is injecting reactive power via a synchronous generator. The excitation system utilizes an automatic voltage regulator (AVR) control loop to achieve reactive power control for the synchronous generator. The faster and more accurate this AVR control loop is, the faster the voltage fluctuations dampen. This paper utilizes a novel hybrid controller, incorporating the numerical method known as the coefficient diagram method (CDM) and optimization techniques based on laws, algebraic calculations, and constraints. Additionally, it incorporates the Turbulent Flow of a Water-based Optimization Algorithm (TFWO) and a robust hybrid objective function to effectively control the AVR system. In this control method, water flow turbulence algorithm is employed to adjust the parameters of the proposed control. To show the efficiency of the proposed control strategy, it has been tested and compared on a standard system. The proposed strategy outperforms other methods in terms of performance criteria measured in both the time and frequency domains. The figures and numerical results demonstrate this superiority. Furthermore, unlike other approaches, this strategy does not necessitate resetting the control parameters obtained at the operating point. The results also emphasize the high speed, stability, and robustness of the suggested method.

Keywords: Automatic voltage control (AVR), Coefficient diagram method (CDM), Turbulent Flow of Water-based Optimization Algorithm (TFWO), Coronavirus 2019 (COVID-19).

Graphical Abstract



Nomenclature

AVR	Automatic Voltage Regulator	y	Output of the controlled system
K_p	The PID controller's proportional gain	a_i	Coefficients of characteristic polynomial
K_i	The PID controller's Integral gain	Y_i	Stability indices
K_d	The PID controller's Derivative gain	τ	Equivalent time constant
K_a	The gain of an amplifier	T_s	Settling time (sec)
K_e	The gain of an exciter	OS	Peak overshoot
K_g	The gain of a generator	US	Peak undershoot
K_s	The gain of a sensor	MDR	Minimum damping ratio
τ_a	The amplifier's time constant	IAE	Integral of absolute error
τ_e	The exciter's time constant	$ITAE$	Integral of time multiplied absolute error
τ_g	The generator's time constant	ISE	Integral of squared error
τ_s	The sensor's time constant	$ITSE$	Integral of time multiplied squared error
ΔV_t	Incremental change in terminal voltage	TFWO	Turbulent Flow of Water-based Optimization
ΔV_{ref}	Incremental change in reference voltage	X_i	The location of the i -th whirlpool within the TFWO algorithm
CDM	Coefficient diagram method	FE	Centrifugal force
$N(s)$	Numerator of transfer function of open loop plant	x_p^{max}	The maximum limit in the D-th dimension in TFWO algorithm
$D(s)$	Denominator of transfer function of open loop plant	x_p^{min}	The minimum limit in the D-th dimension in TFWO
$A(s)$	Forward denominator polynomial of CDM	Δx_i	The degree of deviation of objects
$B(s)$	Feedback numerator polynomial of CDM	Wh_i	The location of the i -th whirlpool within the TFWO algorithm
$F(s)$	Reference numerator polynomial of CDM	N_p	The quantity of populations involved in the TFWO algorithm
r	Reference input	N_{wh}	The count of whirlpools within the TFWO algorithm
u	The signal generated by the controller	δ	Rotation angle of objects
d	The signal representing an external disturbance	ΔWh_i	The degree of deviation of whirlpools

Introduction

The new coronavirus (SARS-CoV2) was first detected in December 2019 in Wuhan, China. A new infectious disease called COVID-19 spread rapidly in China and then around the world [1]. The virus has been defined by the World Health Organization (WHO) as an epidemic and has affected most parts of Europe, the Americas, and Asia [2,3]. Ministry of Health Governments have declared red status and ordered home quarantine in some cities to reduce the incidence and mortality of COVID-19, and in some countries, even the commercial and industrial sectors were closed. This home quarantine trend has drastically reduced electricity demand and changed the pattern of load consumption and daily load characteristics. These abrupt changes in the consumption pattern, imposed on electricity companies and the distribution system due to special circumstances, have created a new challenge in supplying energy to consumers. This new challenge has caused voltage fluctuations, increased losses, and imbalances in the power system [4,5].

Shifting the electricity demand pattern has caused problems in voltage regulation in some areas of the power system [6]. Reducing the consumption of some consumers during the day and increasing the distributed generation (DG) sources' penetration in the power system has led to an increase and fluctuation of voltage in the power system [4,7]. This is especially the case in some local areas with large numbers of factories and commercial buildings that have been completely or partially shut down during the outbreak of COVID-19. The alteration in real power demand impacts the frequency, whereas the modification in reactive power primarily influences the magnitude of voltage [5,6]. This increase in voltage fluctuations due to reduced load consumption and prolonged low power demand must be offset by some sources. Because voltage control in the power system is mostly realized by reactive power, some power sources must be exploited in the power system that can control voltage fluctuations. These techniques encompass the utilization of generators, static reactive power compensators (SVCs), flexible alternating current transmission system (FACTS) devices, capacitors, and reactors [8–10]. Reactive power control and reduction of generator terminal voltage fluctuations are carried out by controlling the reactive power of the generators and by regulating the excitation current and excitation field. To this end, the amount of reactive power injected into the power system and, finally, the voltage can be controlled using a generator's excitation system. These methods involve employing generators,

static reactive power compensators (SVCs), flexible alternating current transmission system (FACTS) devices, capacitors, and reactors [11,12]. The purpose of an automatic voltage regulator (AVR) is to maintain the voltage at the designated level at the synchronous generator terminal by injecting reactive power through the generator.

The automatic voltage regulator (AVR) control loop is considered one of the fundamental control loops within a power plant. Due to the fact that instability in the automatic voltage regulator (AVR) can result in instability of the entire power system, the performance of its control system is exceptionally sensitive [13]. This system receives its signals from different parts and generates the AVR control signal. This signal is to reduce the voltage error, and all limiters have acted on it, i.e., the control signal is calculated so that none of the limits are neglected [14].

In recent times, numerous controllers have been explored by researchers to address the issue of automatic voltage control in power systems and enhance the system's response. Among these controllers are proportional-integral-derivative (PID) controllers, fuzzy logic-based controllers, robust controllers, and controllers based on neural networks. These controllers are developed using nonlinear and robust techniques, as well as heuristic and metaheuristic intelligent algorithms.

In [15], the nonlinear and robust control method (H_2/H_∞) is used to design the AVR controller. The linear matrix inequality (LMI) technique has been used to solve the issue of constrained optimization and maintain system stability. In [16], the investigation focuses on the fractional-order (FO) proportional-integral-derivative (PID) controller applied to the AVR system. The AVR system's performance criteria are defined as perturbations within the system and subsequently optimized using the multi-objective differential evolution (MODE) optimization algorithm to achieve multiple objectives. The hybrid controller used is combined with the H_2/H_∞ method. In [17], H_∞ robust control method μ -analysis are used to control AVR. This study considers the uncertainty associated with the system parameters. In [18], to strengthen the performance of the system controller against relatively severe disturbances caused by the load, a PI controller with state feedback with two degrees of freedom (2-DOF) is presented, in which the controller coefficients are adjusted by particle swarm optimization (PSO) algorithm. The researchers in reference [19] propose a controller called the interval type-2 fractional order fuzzy PID (IT2FO- FPID) controller. A novel approach is introduced, which combines a type 2 Takagi-Sugeno-Kang (TSK) fuzzy logic controller (IT2FLC) with a PID

fractional-order controller. This combined controller aims to effectively handle uncertainties in the nonlinear operation of the system. In [20], to determine the optimal parameters of an AVR (Automatic Voltage Regulator) PID controller, a hybrid model is employed. This model integrates genetic algorithm (GA), radial basis function neural network (RBF-NN), and Sugeno fuzzy logic. In [21], the AVR generator controller utilizes a fractional-order model reference adaptive controller (FOMRAC). The AVR generator controller utilizes a fractional-order model reference adaptive controller (FOMRAC). In [22], the AVR system integrates a fuzzy controller that automatically adjusts itself. To enhance performance, the scaling factors in this controller are optimized using the PSO algorithm. An online adaptive optimization controller is designed in [23] to optimize AVR performance. To solve the optimal control problem, quadratic optimization using the Adaptive Dynamic Programming (ADP) method is employed. Reference [24] utilizes a combination of a fuzzy controller PID and a programmable logic controller (PLC) to regulate the generator terminal voltage through the AVR system. In reference [25], an AVR system employs a fuzzy logic-based controller optimizing the Fuzzy P + Fuzzy I + Fuzzy D (FP + FI + FD) controller using a hybrid algorithm. The scaling factors of the fuzzy system control are determined using the hybrid GA- PSO (HGAPSO) algorithm. Reference

[26] implements a FOPIAD μ fractional-order controller for the AVR system. The fractional-order control parameters are adjusted by incorporating the improved chaotic genetics II algorithm. In [27], two controllers are exploited to automatically adjust the generator voltage simultaneously. These two controllers are designed based on fuzzy set and type 2 fuzzy logic combined with the PI controller. Ref. [28], uses a self-adjusting PID fuzzy controller for the AVR system and proper performance against uncertainty. Additionally, the TLBO optimization algorithm is applied to enhance the suggested control efficiency. Reference [29] employs a robust control design method to create a controller for the AVR + LFC (Automatic Voltage Regulator + Load Frequency Control) system. In this paper, the nonlinear threshold accepting (NLTA) method and nonlinear NP problem solution in a short time have been used to adjust the control parameters. Moreover, metaheuristic methods such as PSO [30], hybrid GA-bacterial foraging optimization (GA-BF) [31], Manta ray foraging optimization algorithm (MRF) [32], JAYA optimization algorithm [33], Cuckoo optimization algorithm (COA) [34], symbiotic organisms search algorithm (SOSA) [35], Whale Optimization Algorithm (WOA) [36], and Tree

Seed Algorithm (TSA) [37] the design of optimal parameters for the PID controller in the synchronous generator's AVR system utilizes these approaches. Reference [34] proposes the utilization of a chaotic multi-objective method to design a fractional-order PID controller for the AVR system. This manuscript focuses on considering the linear model of the system. The fuzzy controller method optimized with the PSO algorithm is presented to improve the voltage stability in the generator excitation system in AVR [38].

The industrial sector has shown increased interest in classic controllers like PID, primarily because of their straightforward structure and convenient implementation. Because the adjustment of the PID and classical controller coefficients depends on the operating point of the system, and these controllers are usually adjusted in the same operating conditions. Furthermore, the power system poses challenges such as time delay, high order, the nonlinearity of system elements, parameter uncertainty, diverse operating conditions, unexpected power system disturbances, and uncertainties in modeling reactive power changes, as mentioned in reference [39]. Besides, by changing the system conditions, it is impossible to change the PID coefficients quickly and simultaneously, and the parameters of these controllers are obtained based on trial and error in nominal operating points and do not have a specific method with mathematical support. Although it is the simplest and cheapest control method available in the industry, it is not robust against the above conditions. Hence, in recent years, there has been a research emphasis on developing controllers that can deliver optimal performance for the power system amidst varying system parameters and machine conditions. Consequently, to tackle the challenges of robust design and performance in the face of uncertainties, novel control strategies have emerged. These strategies are built upon more advanced approaches such as adaptive control, robust control, predictive control, sliding mode control, and state feedback control, as well as incorporating fuzzy logic and neural networks. Some approaches even combine multiple methods to achieve better outcomes. Although these methods certainly provide better results than classical control, they have very complex processes and calculations and require comprehensive and accurate information from the control system, including information about all state variables; hence they have not become widely applicable in the industry. On the other hand, given the increasing complexity of power systems, restructuring, and economic concepts such as the electricity market, there is a need for novel, robust, yet achievable control

strategies.

To address the issues outlined in this paper, a novel controller named CDM has been employed as a solution. This control strategy divides the previous methods into two categories, i.e., classical or modern, and by introducing a new method, it is in a third category called algebraic methods. Although this control strategy is new, it has been used in the industry for about 40 years to control servo motors, spacecraft, gas turbines, etc., and has been addressed in power engineering and control scientific papers for the last few years [40–44]. These papers indicate a better response to this controller than controllers such as predictive and classical controllers. This method offers several notable features and advantages. It utilizes algebraic polynomials to represent both the system and the controller, employs a control system structure with two degrees of freedom (2DOF), achieves a system step response without overshoot or with minimal overshoot, leverages robust mathematical principles for indirect pole placement in the closed-loop system, and enables a rapid settling time to attain the desired robust response. These characteristics contribute significantly to the effectiveness and benefits of this approach. Consequently, the controller designer can evaluate and estimate the speed, stability, and robustness of the controlled system. These three crucial performance indicators hold significant value in assessing the controllers, making them a notable advantage of this method. Implementing these indicators straightforwardly or even achieving them at all may pose challenges or be unattainable in other methods. In addition, the method of designing the CDM controller is extremely rational and easy to comprehend. It also has a straightforward structure and straightforward calculations that are not difficult to implement. Because of these characteristics, the CDM controller is a strategy that is accurate, practicable, and dependable in the industry.

Nevertheless, with the salient advantages of CDM controllers, there are challenges, such as designing the key parameters of it, i.e., stability index and equivalent time constant. Adjustment of these two parameters is according to the objectives required for the stable operation of this controller, which has been discussed and researched in many studies, and various ranges have been introduced to determine and adjust them [42]. However, the proposed methods lack a clear process, and it is not determined for what values the best performance is achieved. Thus, in order to surmount these challenges and achieve optimal values, this paper introduces the novel TFWO algorithm, which incorporates a robust objective function for the first time. In essence, the novelty

of this paper lies in the introduction and enhancement of the CDM algebra controller's performance by optimally designing its key parameters in accordance with mathematical principles and governing limits. Consequently, a hybrid (algebra-optimal) CDM controller is devised for the AVR system, marking the first instance of its implementation through a novel algorithm. Subsequently, the controller coefficients are calculated for the automatic voltage regulation system. This new algorithm, which is inspired by the whirling flow of water, is proposed to solve the optimization problem. Considering the No Free Lunch (NFL) theory [45], which states that no single algorithm can effectively address all engineering and optimization problems, this paper introduces a novel algorithm to tackle the specific challenges at hand. The proposed algorithm provides advantages such as easy implementation, low parameter adjustment, crossing local minima, fast convergence, high exploration, and exploitation, and searching for finding the optimal solution. Additionally, the proposed objective function aims to design a multi-objective CDM controller by utilizing the weighted coefficient method, where the coefficients are summed accordingly. The functions in question are represented in the form of ITSE criteria, which prioritizes errors with greater magnitudes and longer durations within the system. The aims include minimizing the controller output signal to avoid saturation, reducing costs, achieving faster settling time and the peak time for improved response speed, and increasing the minimum damping ratio (MDR) of the system to enhance the stability and robustness of the designed controller. These functions have become a comprehensive objective function using the sum of weighted coefficients methods.

To show the efficiency of the proposed control strategy when faced with load step changes and uncertainties due to large changes in dynamic values, it is tested on the sample system. Moreover, using the classic PID controller of [8], the desired performance indices in both time and frequency domains are compared. The figures and numerical data exhibit the superiority of the proposed control strategy through various performance criteria, including overshoot, undershoot, peak-to-peak, settling time, ITSE, and the MDR. In general, the main objectives and contributions of the paper can be listed as follows:

- The paper introduces and enhances a combination of the CDM algebra controller with a powerful mathematical back up and optimizing its key parameters according to all mathematical rules and its governing limits and, as a result, designing a hybrid (algebra- optimal) CDM controller for the AVR system for the first time.

- The CDM controller's key parameters are optimized by employing a novel algorithm incorporating a combined objective function. This objective function aims to minimize the ITSE, the controller output signal, the settling time, and the peak time while simultaneously increasing the MDR.

- It is essential to utilize qualitative and quantitative data in both the time and frequency domains to demonstrate the superiority of the suggested control technique. This is particularly important when addressing load step changes and uncertainties arising from significant variations in dynamic values.

The paper is structured as follows: Section 2 provides an overview of the AVR system modeling, including the description of transfer functions. Section 3 discusses the design of the CDM controller, accompanied by an explanation of the TFWO algorithm and

the objective function. In Section 4, the simulation results of the proposed method applied to the AVR system are presented, analyzed, and summarized in two subsections. Finally, the paper concludes with the overall findings and conclusions.

The AVR System Modeling

The AVR loop ensures voltage stability within the power system. The AVR system, which plays a crucial role in the power system, consist of four primary components: an amplifier, an actuator, a generator, and a sensor [8,17,18]. A voltage sensor constantly measures and transmits the terminal electrical potential difference. The voltage waveform undergoes rectification and smoothing within a comparator, where it is compared to a direct current (DC) signal source. Subsequently, the error voltage derived from the comparator output is enhanced by an amplifier. Ultimately, this signal is utilized to regulate the excitation of the generator field winding. Figure 1 illustrates the actual model of the AVR system.

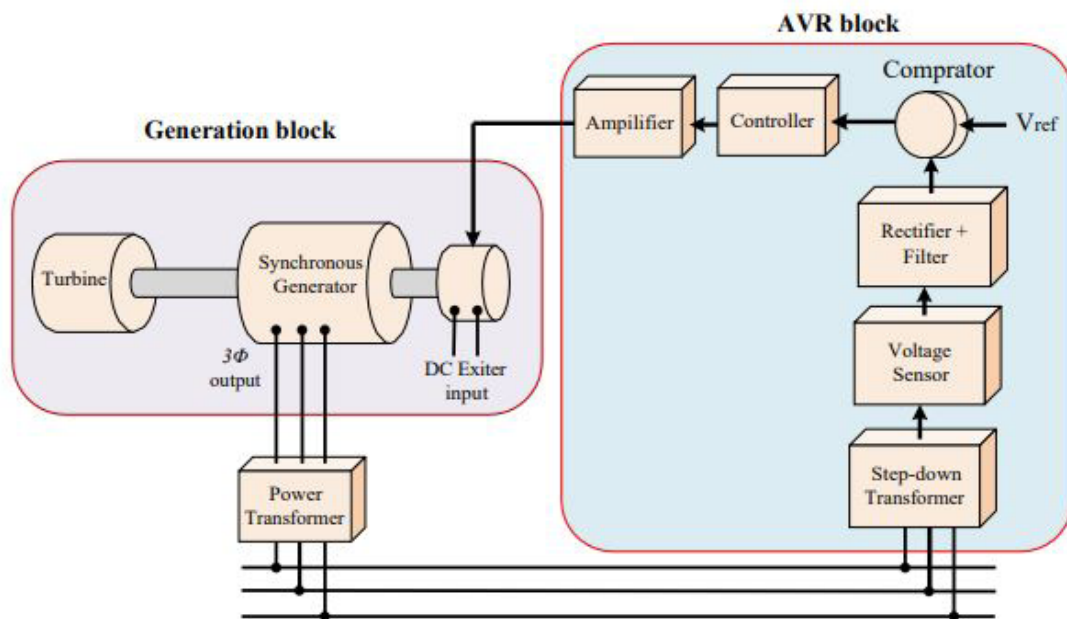


Figure 1: The practical representation of the AVR system

This Figure demonstrates that six components of a basic AVR system, including an amplifier, an exciter, a generator, a sensor, a comparator, and a controller. Based on the information presented in Figure 1, the transfer functions of various components within

the AVR system are outlined below:

The Transfer Function of the Amplifier

The amplifier's transfer function is represented by Eq. (1), where it is modeled using a gain and a time constant [18].

$$G_{\text{Amplifier}}(S) = \frac{K_A}{1 + S\tau_A} \quad (1)$$

The parameters K_A and τ_A in the equation represent the gain and time constant of the amplifier system, respectively. The value of K_A typically falls within the range of 10 to 40, while the time constant τ_A varies between 0.02 seconds and 0.1 seconds.

$$G_{Exciter}(S) = \frac{K_E}{1 + S\tau_E} \quad (2)$$

The Transfer Function of the Generator

The transfer function for the terminal voltage of the generator is represented by Equation (3) [18].

$$G_{Generator}(S) = \frac{K_G}{1 + S\tau_G} \quad (3)$$

The parameters K_G and τ_G denote the gain and time constant of the generator model, respectively. The value of K_G falls within the range of 0.7 to 1.0, while the time constant τ_G varies between 1.0 and 2.0.

$$G_{Sensor}(S) = \frac{K_S}{1 + S\tau_S} \quad (4)$$

The parameters K_S and τ_S represent the gain and time constant of the sensor model, respectively. The value of K_S ranges from 0.9 to 1.1, while the time constant τ_S varies between 0.001 and

The Transfer Function of the Exciter

The transfer function of the exciter is represented in a similar manner to that of the amplifier, utilizing a gain and a time constant, as illustrated in Equation (2) [18].

The Transfer Function of the Sensor Component

The transfer function of the sensor is represented by Equation (4), where it is modeled using an increment and a time constant [18].

0.06. Figure 2 presents the block diagram of the AVR system, depicting the arrangement of components based on Figure 1 and the transfer functions associated with each component.

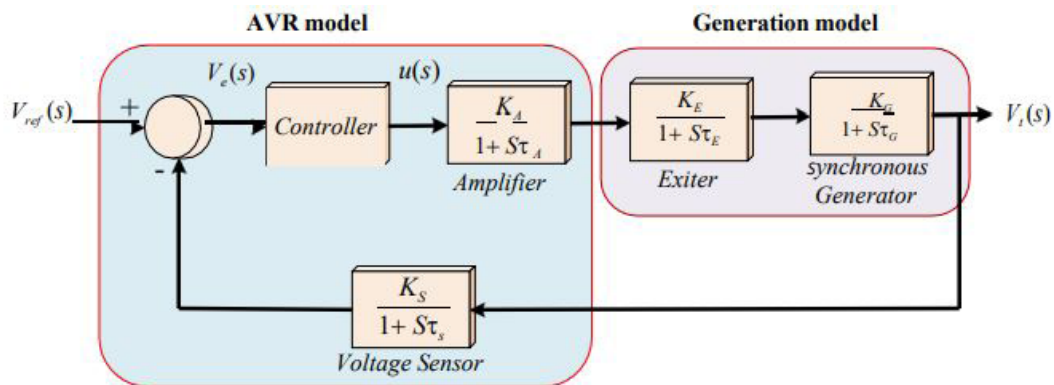


Figure 2: The block diagram of AVR system

Design of the AVR System Controller

Coefficient Diagram Method

In 1991, Professor Shunji Manabe introduced the coefficient diagram method (CDM), which is an algebraic approach that utilizes polynomial expressions to mathematically represent a system [46]. Polynomial representation of the controller and plant are used in this method. To achieve this objective, a control system structure with two degrees of freedom (2DOF) is employed, ensuring the absence of any significant overshoots. Furthermore, unlike optimal controllers, CDM leverages a robust mathematical framework to facilitate pole placement and indirectly determine the settling time. Through this, a desirable robust controller is designed and desirable response is obtained. Thus, speed, stability and robustness, which are the three key parameters in controller designing are gained. This can be considered as a major advantage of this method, which is pretty unique. The methodology for the design is flawlessly scientific and effective, and the execution is straightforward. Because of it,

the CDM-based controller may now serve industrial purposes with increased precision, viability, and dependability. [46, 47].

In CDM, there is a tool called as "Coefficient Diagram" that is quite helpful and powerful. This tool, along with Bode and Nyquist diagrams, is applied in the process of designing controllers. By examining this particular figure alone, we can obtain valuable insights into the time response speed, stability, and robustness criteria. The convexity level of a curve may be established by analyzing the coefficients of the feature's polynomial in conjunction with the curve's overarching tendency. The extent to which the ai curve shifts in response to variations in the plant's parameters serves as an indicator of the system's stability, response speed, and resilience. The necessary condition for stability may be precisely calculated by using this diagram in conjunction with the Routh criterion for lower orders and the Lipatoy criteria for higher orders [48]. Figure 3 illustrates the block diagram representation of a single-input, single-output (SISO) system employing the CDM.

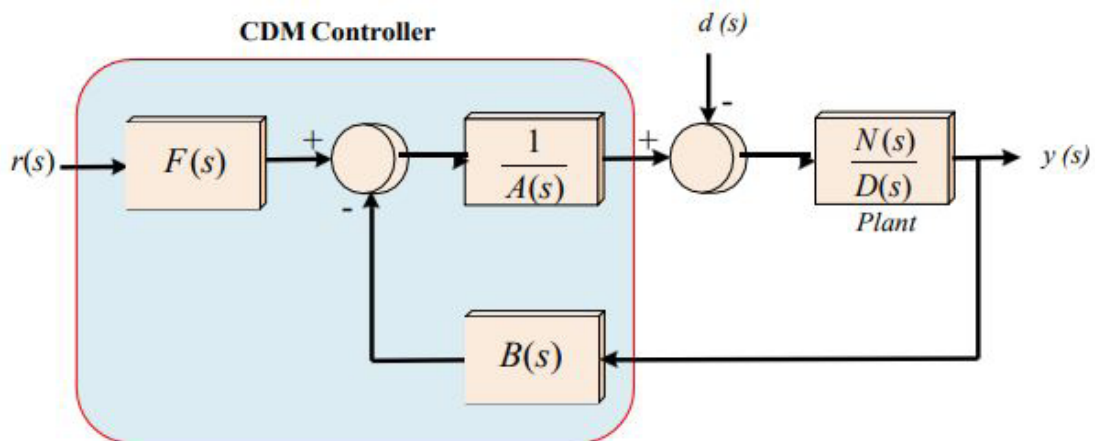


Figure 3: The block diagram of the structure of CDM controller

The presence of two numerators in the controller's transfer function signifies a two-degree-of-freedom (2DOF) structure. By utilizing a two-degree-of-freedom (2DOF) structure, the

focus can be directed toward addressing disturbances and tracking the reference signal. The output of the controller system is expressed as follows:

$$y = \frac{N(s)F(s)}{P(s)}r + \frac{A(s)N(s)}{P(s)}d \quad (5)$$

Whereby, the characteristic polynomial of the closed-loop system is denoted by P(s), and it is defined as follows:

$$P(s) = A(s)D(s) + B(s)N(s) \tag{6}$$

The following gives A(s) and B(s).

$$A(s) = \sum_{i=0}^n l_i s^i \quad \text{and} \quad B(s) = \sum_{i=0}^q k_i s^i \tag{7}$$

For practical reasons, p>=q is an essential condition and by substituting (7) in (6), P(s) is obtained:

$$P(s) = \sum_{i=0}^p l_i s^i D(s) + \sum_{i=0}^q k_i s^i N(s) = \sum_{i=0}^n a_i s^i, \quad a_i > 0 \tag{8}$$

Determining the parameters τ and Y_i is a critical factor in the design of the CDM controller. The parameter τ affects the magnitude of the control signal and the speed of the system.

The stability and shape of the time response are determined by the parameter Y_i . The parameters and a_i exhibit the following variations:

$$\gamma_i = \frac{a_i^2}{a_{i+1}a_{i-1}}, \quad i \in [1, n-1], \quad \gamma_0 = \gamma_n = \infty \tag{9}$$

$$\tau = \frac{a_1}{a_0} \tag{10}$$

$$\gamma_i^* = \frac{1}{\gamma_{i-1}} + \frac{1}{\gamma_{i+1}}, \quad i \in [1, n-1] \tag{11}$$

Based on the standard form of S. Manabe, Y_i values can be {2.5, 2, 2...2} that can lead to desirable performance. Stability indices are determined as $Y_i=1.5\sim 4$ too, which is due to Routh and Lipatov's criteria of stability. Results have shown that stability is

guaranteed and all poles are negative when $Y_i > 1.5Y_i^*$ and all of $Y_i > =1.5$. These standards indicate that to have an acceptable and logical design, τ must be as follows [42]:

$$\tau \approx \frac{1}{3^s} T \tag{12}$$

P_{target} is written as follows:

$$P_{target} = a_0 \left[\sum_{i=2}^n \left(\prod_{j=1}^{i-1} \frac{1}{\gamma_j} \right) (\tau s)^i \right] + \tau s + 1 \tag{13}$$

By setting P(s) equal to Ptarget(s), the coefficients of the A(s)

and B(s) polynomials are determined. In addition, the reference numerators polynomials F(s) are obtained as follows:

$$F(s) = \frac{(P(s)|_{s=0})}{N(s)} \tag{14}$$

TFWO Algorithm

The TFWO algorithm was originally introduced by Ghasemi et al. in their publication [49]. The inspiration behind this optimization approach stemmed from the turbulent flow observed in water. The core of the whirlpool behaves in a manner like to that of a sink or a vacuum by drawing nearby objects and particles into its center and farther into the vortex. This action may be seen as the application of centrifugal force to the particles. This force is ultimately overcome by the centrifugal force. The centripetal and centrifugal forces that were acting upon the particle are shown in Fig. 4 (a). Several stages, including the following, are represented for the TFWO algorithm:

- The influence of whirlpools on the objects and particles that are a member of their set as well as the set of other whirlpools

- The process of establishing the whirlpool (NWh: a collection of whirlpools)
- The force of centrifugal acceleration

The interactions between individual whirlpools

- **The beginning of the construction of the whirlpool (NWh: a group of whirlpools)**

The algorithm's starting population, denoted by N_p , is evenly distributed across the NWh groups, also known as whirlpools. Then, the member of the population of each whirlpool (Wh) with the highest strength is chosen to serve as the center or sink of that whirlpool. This causes the objects and particles (X) to be pulled toward the whirlpool center in proportion to how close they are to the center.

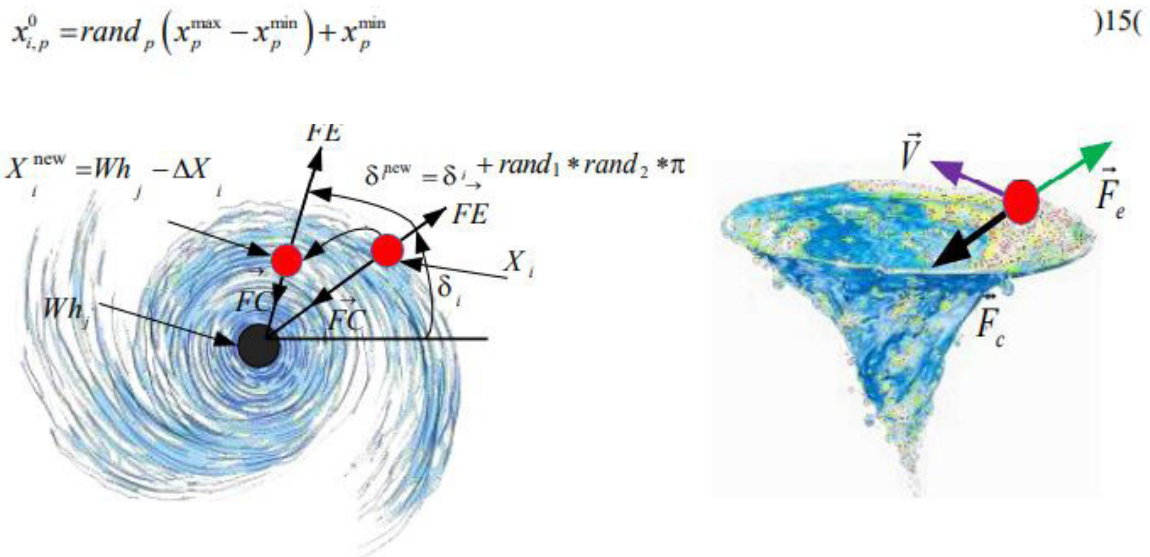


Figure 4: A whirlpool that is formed by (a) a centripetal force that is caused by rotating motion, and (b) the action of centrifugal force, as well as the updating of the locations of particles

- **The impact of whirlpools on the items and particles that are a component of the whirlpool's set as well as those of other things and particles**

When an item is sucked up by the whirlpool, its position and that of the whirlpool become the same, which is when the updating vector of particle positions takes effect; this is represented by the equation $X_i = Wh_j$. Other whirlpools, on the other hand, may deviate items from their location and absorb them dependent on where they are and how much suction strength they have, which is given by the objective value ($f(Wh_j)$). The value demonstrates

the extent of this discrepancy. Therefore, the j th item, which was located at X_i , moves as a result of the centripetal force exerted by the whirlpool Wh_j , and the displacement of the object as a result of the other whirlpools is ΔX_i . The parameter that represents the rotation angle of the particle in the updating vector is denoted by the letter, and its value is modified after each iteration. The procedure for upgrading is shown in Fig. 4 (b).

$$\Delta_{t=1:N_{Wh}} = f(Wh_t) * |Wh_t - sum(X_i)|^{0.5} \quad (16)$$

$$\begin{cases} Wh = Wh & \text{if } \Delta_t^{\min} \\ Wh' = Wh & \text{if } \Delta_t^{\max} \end{cases} \quad (17)$$

$$\delta_i^{\text{new}} = \delta_i + rand_1 * rand_2 * \pi \quad (18)$$

$$\Delta X_i = \cos(\delta_i^{\text{new}}) * (Wh_f - X_i) - \sin(\delta_i^{\text{new}}) * (Wh_w - X_i); \quad (19)$$

$$X_i^{\text{new}} = Wh_j - \Delta X_i; \quad (20)$$

• Centrifugal force

When things move into a whirlpool under the influence of a centrifugal force, another force that is also called centrifugal force (FE) is applied to the item, and it causes the object to move away from the vortex. When this happens, the item moves to a

new location as a result of the centrifugal force, which is larger than both the tension and the centrifugal force. Calculations of centrifugal force and the impact of centrifugal force may be found by using the following equations:

$$FE_i = \left(\left(\cos(\delta_i^{\text{new}}) \right)^2 * \left(\sin(\delta_i^{\text{new}}) \right)^2 \right)^{1/2}. \quad (21)$$

$$\begin{cases} p = \text{round}(1 + rand * (D - 1)); \\ \text{if } rand < FE_i \left\{ \begin{array}{l} x_{i,p} = x_p^{\min} + x_p^{\max} - x_{i,p} \\ f(X) = f(X_i^{\text{new}}); \end{array} \right. \\ \text{otherwise} \end{cases} \quad (22)$$

• The whirlpools' interactions with one another whirlpools

The whirlpools interact with one another and produce movement in both of themselves, in addition to the impact that the whirlpool has on the items. This movement is analogous to

the movement of items toward a whirlpool, and any vortex that has a more powerful centrifugal force will move the whirlpool around it and swallow it up. Following are some formulae that may be used to compute the displacement of nearby whirlpools in relation to one another:

$$\Delta_{t=1:N_{Wh}-\{j\}} = f(Wh_t) * |Wh_t - sum(Wh_j)| \quad Wh_f = Wh \quad \text{with minimum value of } \Delta_t \quad (23)$$

$$\delta_j^{\text{new}} = \delta_j + rand_1 * rand_2 * \pi. \quad (24)$$

$$\Delta Wh_j = rand(1, D) * \left| \cos(\delta_j^{\text{new}}) + \sin(\delta_j^{\text{new}}) \right| * (Wh_f - Wh_j); \quad (25)$$

$$Wh_j^{\text{new}} = Wh_f - \Delta Wh_j; \quad (26)$$

Defining the Optimization Problem and Objective Function

Obtaining key parameters is an essential step in the process of constructing a CDM controller, as was previously indicated. In the earlier references, the selection of these parameters is accomplished via trial and error; there is no particular mathematical technique involved. In addition, it is not quite obvious if the key parameters lead to the best feasible outcomes. Therefore, to solve these problems, this paper attempts to apply an optimal- algebraic CDM controller for the AVR system for the first time. The smart combination of algebraic CDM and optimization methods considering all of its mathematical

rules is used in the proposed controller. Therefore, to design a powerful controller with fast response and maximum stability, an optimization problem is defined and four objective functions are considered as follows.

- *The ITSE index for voltage variations*

There are several indices in the design of controllers, including ITAE, IAE, ITSE, and ISE, each of which has advantages. However, the ITSE index takes precedence as the primary objective function due to its incorporation of the advantages of other indices while also ensuring a rapid dynamic response. This objective function for the AVR system is defined as follows:

$$f_1 = ITSE = \int_0^t (V_e(t))^2 \cdot dt \quad (27)$$

- *Settling time and peak time*

To increase the response speed and reduce its settling time, as well as to reduce the amplitude and peak time, the second objective function is defined as follows:

$$f_2 = Ts_{V_t} + Tp_{V_t} \quad (28)$$

- *Control cost*

By paying any attention to f_2 and f_1 of voltage fluctuations, the response may be made to move at a quicker rate; however, this may result in an increase in control gain. As a consequence of this, raising the control gain is seen as a flaw in terms of controller

$$f_3 = ITSE = \int_0^t (u(t))^2 \cdot dt \quad (29)$$

- *Minimum damping ration (MDR)*

To achieve a more stable response, an objective function is employed, which focuses on maximizing the MDR of all

$$f_4 = 1 - MDR \quad (30)$$

design. In simpler terms, having a lower control gain brings advantages such as prevention of actuator saturation, reduction in the cost of monitoring a larger actuator, and diminishment of the output signal (u). In light of this, the third objective function

eigenvalues. This objective function is referred to as the fourth objective function and is given in the following equation:

Given that there are four objective functions, it is necessary to employ a method that can minimize all of these functions equally and within a single range to solve the optimization problem.

To this end, the sum of the weighted coefficients method for objective functions has been converted into a single objective function. Finally, the general objective function is considered as follows using the sum of weighted coefficients method:

$$F = \sum_{i=1}^4 \alpha_i \omega_i f_i = \alpha_1 \omega_1 f_1 + \alpha_2 \omega_2 f_2 + \alpha_3 \omega_3 f_3 + \alpha_4 \omega_4 f_4 \tag{31}$$

Where ω is are weighted coefficients, the sum of which is equal to one. The α coefficients are utilized to ensure equal weighting of

each term and promote competitiveness among them throughout the optimization process. The optimization problem is defined in this paper as follows:

$$\begin{aligned} & \text{Minimize } F(Y, \tau), \\ & \text{subject to :} \\ & Y_{i, \min} \leq Y_i \leq Y_{i, \max} \\ & \tau_{i, \min} \leq \tau_i \leq \tau_{i, \max} \end{aligned} \tag{32}$$

Applying the TFWO Algorithm to the Optimal CDM Controller

This section describes how to connect and design a hybrid CDM controller and TFWO algorithm. The connection block diagram

of the proposed controller to the AVR system is depicted in Figure 5. Moreover, the algorithm flowchart, along with the calculation of the parameters and objective functions is shown in Figure 6.

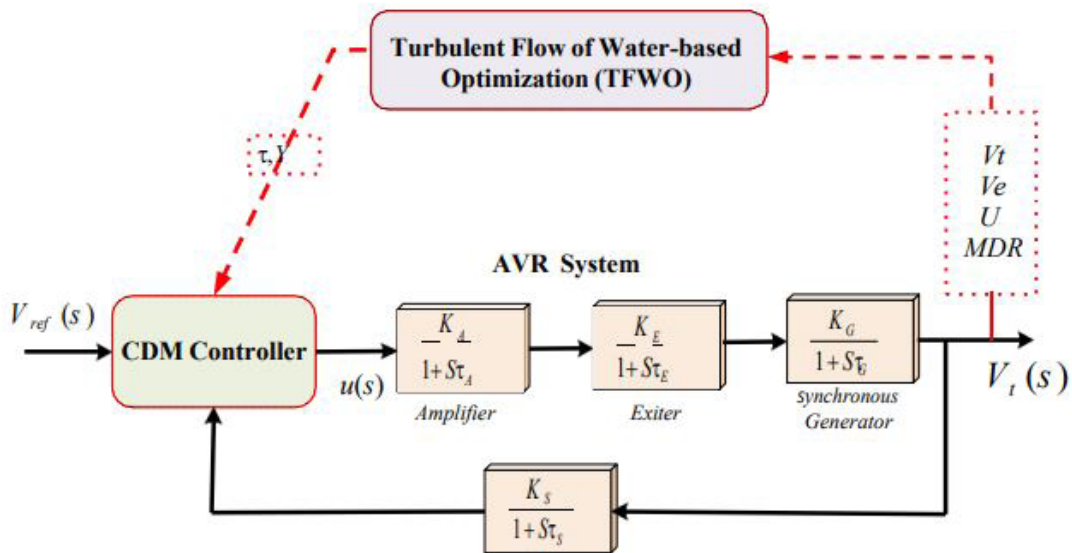


Figure 5: the block diagram of the AVR control system in conjunction with the proposed CDM-TFWO controller

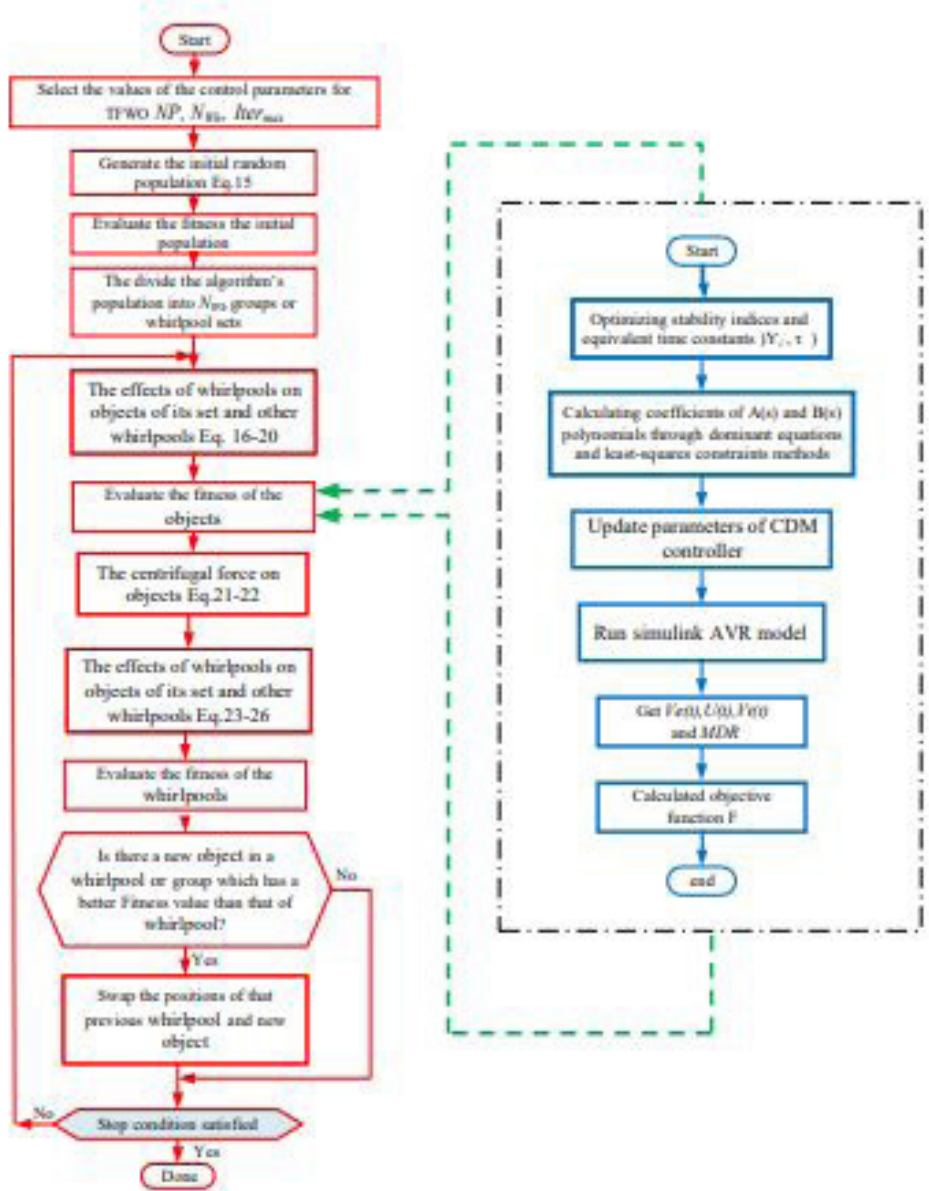


Figure 6: The flowchart of designing the optimal CDM using the TFWO method for the AVR system

Simulation Results

The System Under Study

In this section, the simulation outcomes of implementing the proposed method for AVR control in the generator excitation system are presented, aiming to minimize voltage fluctuations. To this end, the optimized CDM control strategy optimized by the

TFWO is applied to the standard voltage control sample model of Figure 2 and is compared with the classic PID controller in Table 1 [8]. The parameters of the system being analyzed, along with the AVR system within the defined range, are presented in Table 2. Information about the algorithm is also given in the Appendix section of the paper.

Table 1: Coefficients of the reference PID controller [8]

K _P	K _I	K _D
1	0.25	0.28

Table 2: Parameters of the AVR system model

	Transfer function	Parameter limits	Used parameter values
Amplifire	$K_a/(1+s\tau_a)$	$10 \leq K_a \leq 40, 0.02 \leq \tau_a \leq 0.1$	$K_a=10, \tau_a=0.1$
DC Exciter	$K_e/(1+s\tau_e)$	$1 \leq K_e \leq 10, 0.4 \leq \tau_e \leq 1.0$	$K_e=1, \tau_e=0.4$
Generator	$K_g/(1+s\tau_g)$	$0.7 \leq K_g \leq 1.0, 1.0 \leq \tau_g \leq 2.0$	$K_g=1, \tau_g=1$
Sensor	$K_s/(1+s\tau_s)$	$K_s=1, 0.001 \leq \tau_s \leq 0.06$	$K_s=1, \tau_s=0.05$

Simulation of the CDM Controller

To adjust the two key parameters of CDM, an optimization method with a new algorithm and a powerful objective function is proposed. Also, a second-order CDM controller (2/2) is used to control the voltage of the test system.

To optimize the parameters Y_i and τ , the transfer function is first linearized and the AVR open loop is extracted in a decentralized way. Then, a combination of CDM algebraic strategy and

optimization is performed according to all the mathematical rules and calculations and governing limits mentioned in the previous section. The optimized parameters are defined within the upper and lower limits as specified in Table 3. After running the algorithm several times and finding the best optimized parameters, the final coefficients related to the forward polynomials and the CDM controller feedback according to the relevant equations in the previous section and the least- squares method is obtained to solve the set of over-determined equations due to degree reduction.

Table 3: Limitation of optimized parameters of CDM

Y_i limitation	2-3
τ_i limitation	0.4-0.7

Figure 7 shows the convergence of the TFWO algorithm and Table 4 lists the optimized final responses. CDM algebraic calculations are also given below. As can be seen, all the relationships governing the CDM control structure are observed and the settling times are optimized in proportion to the equivalent time constant.

Table 4: Optimized key parameters of CDM

Y_1	Y_2	Y_3	Y_4	Y_5	$\tau(s)$
2.0475	2.0349	2.4618	2.1936	2.8168	0.6334

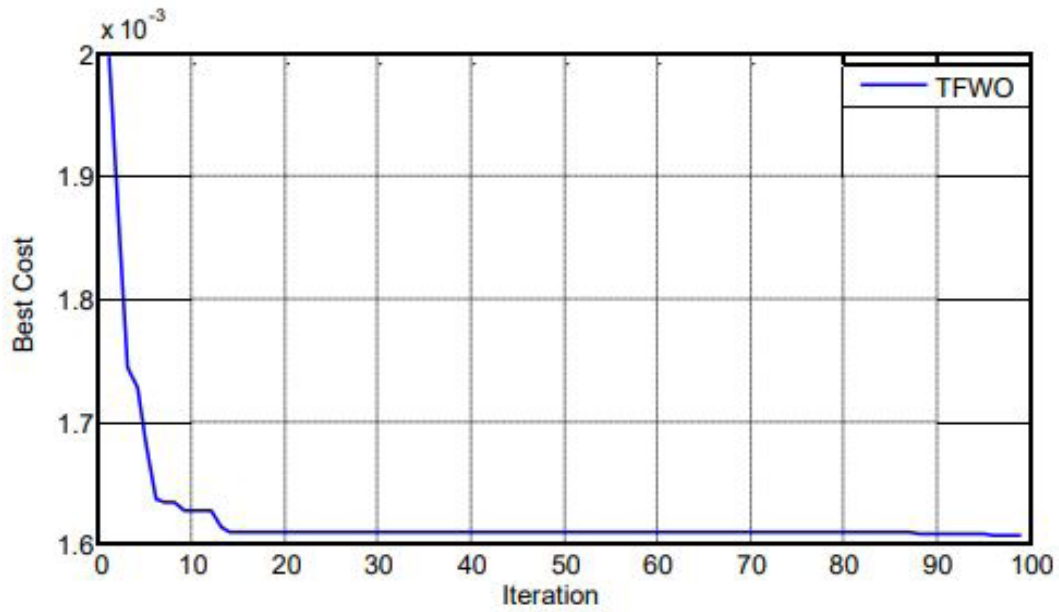


Figure 7: Convergence curve of TFWO for CDM controller

$$\begin{aligned}
 N(s) &= 5000 \\
 D(s) &= s^4 + 33.5s^3 + 307.5s^2 + 775s + 500 \\
 \gamma_i^* &= [0.4914 \quad 0.8946 \quad 0.9473 \quad 0.7612 \quad 0.4559], i \in [1, 5] \\
 P_{\text{target}}(s) &= 0.5175s^6 + 112.3721s^5 + 3342.8s^4 + 29624s^3 + 195940s^2 + 633400s + 1000000 \\
 A(s) &= 0.5175s^2 + 95.0344s \\
 B(s) &= 24.4067s^2 + 117.1766s + 200
 \end{aligned} \tag{33}$$

Figure 8 presents the coefficient diagram, where the horizontal axis represents the order "i" values associated with each coefficient. The related description is provided in the previous sections.

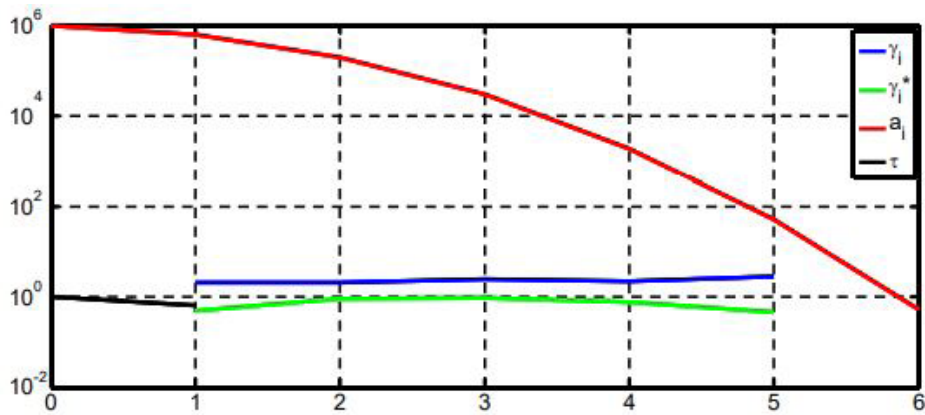


Figure 8: Coefficient diagram of designed proposed controller

Numerical and simulation results in the time and frequency domains obtained by comparing the reference control and the optimal CDM controller strategies proposed in the system under study are shown in Figure 9 and Table 5. According to the graph

and especially the numerical results based on settling time, peak time, and ITSE in less time and higher MDR as a result of the proposed control strategy, it is obvious that optimal CDM offers better performance than the reference classic PID.

Table 5: Numerical comparison of the outcomes of various control techniques

Control strategy	$T_s(\text{sec}), V_t$	$T_p(\text{sec}), V_t$	ITSE (Ve)	Oscillatory modes	MDR (ζ)
PID	1.2604	1.5500	0.0552	$-0.1080 \pm 4.4191i$	0.0244
Optimal CDM	1.0024	1.2300	0.0105	$-2.13e+00 \pm 6.01e+00i$	0.3338

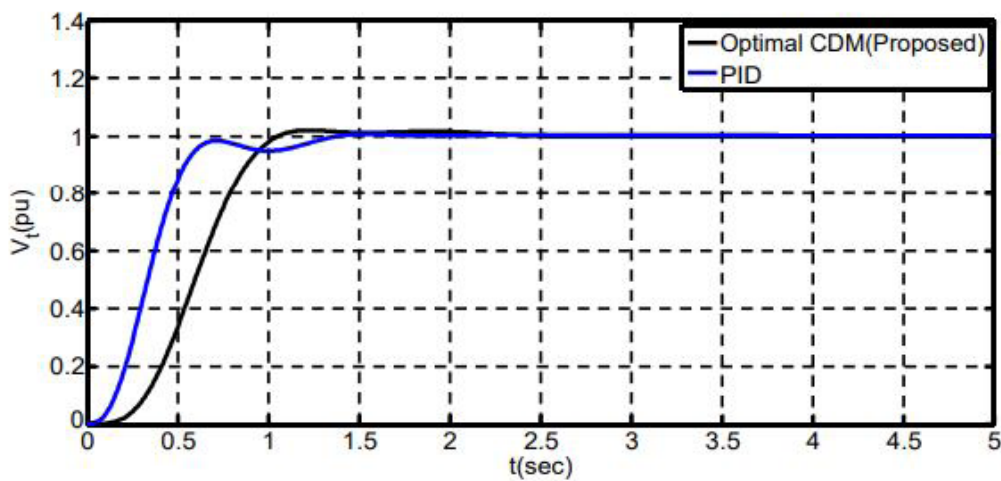


Figure 9: Generator terminal voltage with two strategies: Reference PID control and the proposed optimal CDM

Robustness of the CDM Controller

A sensitivity analysis was carried out to assess the resilience of the proposed optimized CDM control strategy when confronted with variations in the range of dynamic parameters. A comparison was conducted between the two control strategies under the condition of significant variations in all dynamic parameters, ranging from $\pm 50\%$. Numerical results based on the MDR are listed in Table 6 and the step response of AVR is shown in Figure

10. According to the eigenvalue studies, it is obvious that the responses obtained from the optimal CDM control strategies are more stable and robust than the compared PID control strategy due to the higher value of MDR when dealing with uncertainties. It is noteworthy that under the most severe uncertainties studied, the optimal MDM control strategy maintains the stability of the voltage control system under study in terms of positive MDR, while the PID controller has unstable modes with a positive true part and as a result a negative MDR.

Table 6: Sensitivity analysis with changes in the range of dynamic parameters

Parameter variation	Nominal	K_A	T_A	K_E	T_E	K_G	T_G	K_S	T_S
% change	0	+ 5 0 % -50%	+ 5 0 % -50%	+ 5 0 % -50%	+ 5 0 % -50%	+ 5 0 % -50%	+ 5 0 % -50%	+ 5 0 % -50%	+ 5 0 % -50%
MDR_{PID}	0.0244	-0.0643 0.2026	-0.0169 0.0929	-0.0643 0.2026	0.0347 0.0316	-0.0643 0.2026	0.0884 -0.0541	-0.0643 0.2026	-0.0070 0.0636
$MDR_{Optimal\ CDM}$	0.3338	0.1946 0.4251	0.2150 0.5390	0.1946 0.4251	0.3030 0.2412	0.1946 0.4251	0.4136 0.1634	0.1946 0.4251	0.2429 0.4535

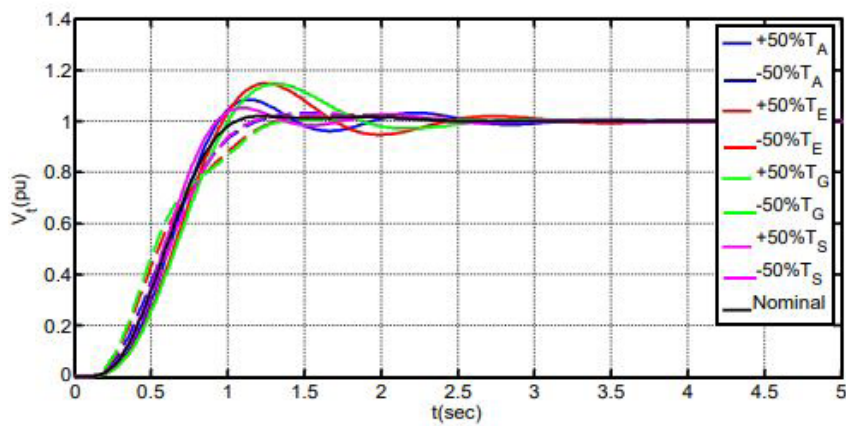


Figure 10: Sensitivity analyses of generator terminal voltage using the proposed CDM control strategy

The remaining sensitivity analysis investigations were conducted by introducing a maximum uncertainty of 50% in all time constants pertaining to the proposed control strategy. Figure 11 illustrates the diagrams and root loci under the specified conditions. The observed insensitivity in this study signifies the robustness of the system, as it maintains consistent dynamic responses even in the face of significant uncertainty. Consequently, once the optimized

parameters of the proposed control strategy are acquired at the operating point, there will be no further need for readjustment. The results of the sensitivity analysis align with the designer's expectations regarding the optimization of key parameters in the CDM controller, highlighting the proposed control strategy's speed, stability, and robustness.

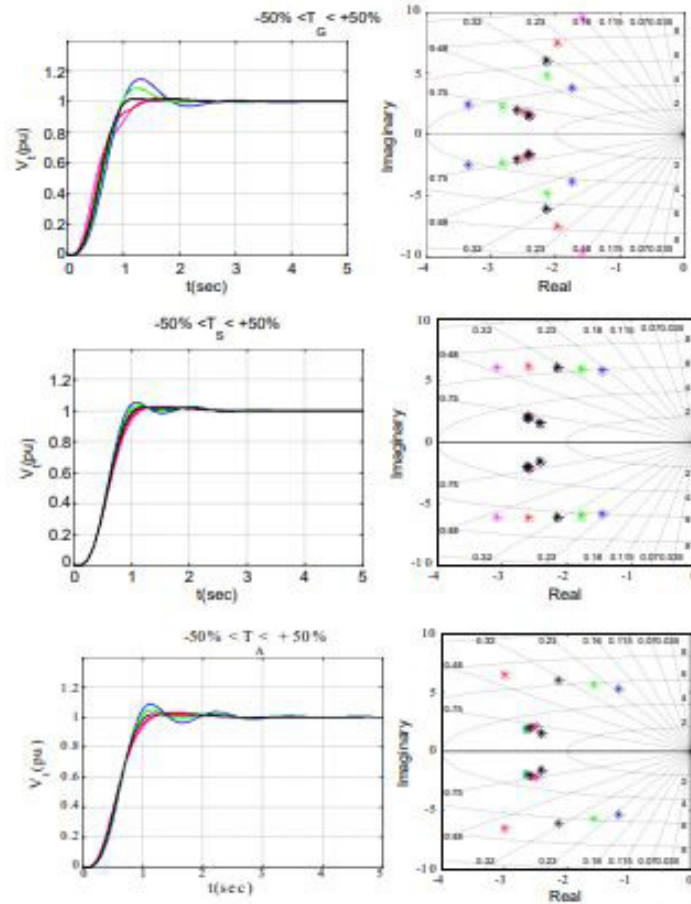


Figure 11: The frequency response of the AVR system, along with the root loci obtained using the optimal CDM control method

Moreover, to indicate the correct performance of the optimized CDM controller against different step changes in reference voltage, the response of the AVR system with the proposed controller

is shown in Figure 12. According to the simulation results, the CDM controller provides a fast and stable performance and also proving the robust performance of the suggested controller against unforeseen changes.

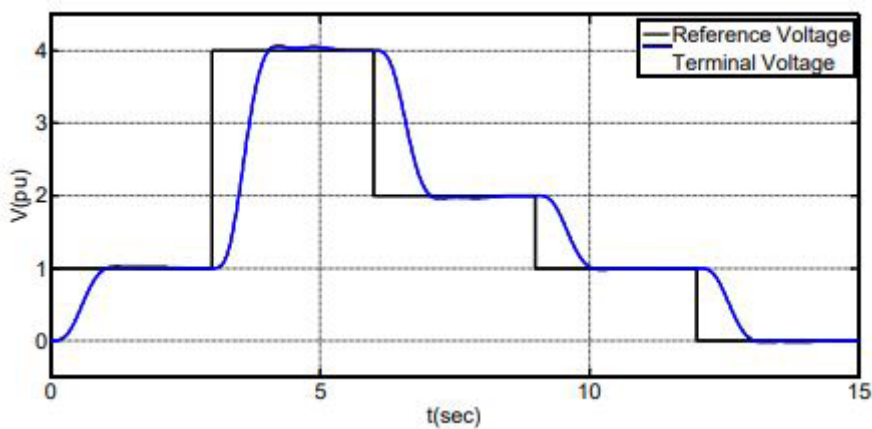


Figure 12: Terminal voltage of the AVR system in response to different step changes in reference voltage

Conclusion

Since the AVR system in voltage control of the generator and stability of power system are of high importance, the proposed method in this paper was studied for the better and more stable control of the AVR system and power system. In this study, a novel approach was employed for the first time, utilizing a combination of an algebraic CDM controller and optimization its key parameters, to regulate the voltage of the generator excitation system. The initial step in optimizing the critical parameters of CDM involved extracting the open-loop transfer function of AVR. Next, the TFWO algorithm was used to perform a combination of algebraic CDM strategy and optimization in accordance with all mathematical rules, calculations, and governing limits. Finally, the CDM critical parameters were optimized. For the optimized parameters, the upper and lower limits were considered reasonable according to the problem formulation. The final coefficients related to the forward and feedback polynomials of the CDM controller were obtained according to the relevant governing equations and the least-squares method to solve the system of over-determined equations due to degree reduction. In this approach, the TFWO algorithm is employed for optimization, which serves as a comprehensive and potent objective function. The primary focus is on reducing the ITSE

criteria over time, enhancing the performance of the controller's output signal, minimizing settling time and peak time, and improving the MDR. The control strategy's effectiveness was demonstrated by conducting simulations on a standard system. The visual and numerical results of generator terminal voltage were obtained for overshoot, undershoot, peak to peak, settling time, peak time, ITSE, and MDR criteria. Responses obtained by the proposed optimal CDM control strategy are faster, more stable, and more robust than those of the reference classic PID controller. Concerning the sensitivity analysis, the optimized parameters of the suggested control strategy, obtained once at the operating point, do not need any additional modifications. Based on the several visual and numerical results in frequency and time domain, this is an accurate, feasible, and reliable strategy to be realized in the industry.

Appendix

Parameters of the AVR System

$KA = 10; TA = 0.1; KE = 1.0; TE = 0.4; KG = 1.0; TG = 1.0; KS = 1.0; TS = 0.05;$

Parameters of the TFWO Algorithm

Max Iterations = 100, Number of search agents = 40

References

1. Organization WH. Coronavirus. WHO (2020) https://doi.org/https://www.who.int/health-topics/coronavirus#tab=tab_1.
2. Buonaguro L, Tagliamonte M, Tornesello ML, Buonaguro FM (2020) SARS-CoV-2 RNA polymerase as target for antiviral therapy. *J Transl Med* 18:185.
3. Ruiz Estrada MA, Park D, Lee M (2020) The Evaluation of the Final Impact of Wuhan COVID-19 on Trade, Tourism, Transport, and Electricity Consumption of China. *SSRN Electron J*.
4. Implications of COVID-19 for the electricity industry: A comprehensive review. *CSEE J Power Energy Syst* 2020.
5. Tsao YC, Thanh VV, Lu JC, Wei HH (2021) A risk-sharing-based resilient renewable energy supply network model under the COVID-19 pandemic. *Sustain Prod Consum* 25: 484-98.
6. Santiago I, Moreno-Munoz A, Quintero-Jiménez P, Garcia-Torres F, Gonzalez-Redondo MJ (2021) Electricity demand during pandemic times: The case of the COVID-19 in Spain. *Energy Policy* 148: 111964.
7. Werth A, Gravino P, Prevedello G (2021) Impact analysis of COVID-19 responses on energy grid dynamics in Europe. *Appl Energy* 281: 116045.
8. Saadat H (1999) *Power system analysis. vol. 2*. McGraw-hill.
9. Belwin Edward J, Rajasekar N, Sathiyasekar K, Senthilnathan N, Sarjila R (2013) An enhanced bacterial foraging algorithm approach for optimal power flow problem including FACTS devices considering system loadability. *ISA Trans* 52: 622-8.
10. Hingorani NG, Gyugyi L (2000) *Understanding FACTS: Concepts and Technology of Flexible AC Transmission Systems*. Wiley.
11. Kundur P, Balu NJ, Lauby MG (1994) *Power system stability and control*. McGraw-Hill.
12. Padiyar KR (2004) *Power System Dynamics: Stability and Control*. Anshan.
13. Gaing ZL (2004) A Particle Swarm Optimization Approach for Optimum Design of PID Controller in AVR System. *IEEE Trans Energy Convers* 19: 384-91.
14. Pan I, Das S (2013) Frequency domain design of fractional order PID controller for AVR system using chaotic multi-objective optimization. *Int J Electr Power Energy Syst* 51: 106-18.
15. Aghaie Z, Amirifar R (2008) An LMI Approach to Robust Controller Design for AVR System. 2008 40th Southeast. Symp. Syst. Theory, IEEE 17-24.
16. Das S, Pan I (2014) On the Mixed H_2/H_∞ Loop-Shaping Tradeoffs in Fractional-Order Control of the AVR System. *IEEE Trans Ind Informatics* 10: 1982-91.
17. Modabbernia M, Alizadeh B, Sahab A, Moghaddam MM (2020) Robust control of automatic voltage regulator (AVR) with real structured parametric uncertainties based on H_∞ and μ -analysis. *ISA Trans* 100: 46-62.
18. Gozde H (2020) Robust 2DOF state-feedback PI-controller based on meta-heuristic optimization for automatic voltage regulation system. *ISA Trans* 98: 26-36.
19. Kumar A, Kumar V (2017) A novel interval type-2 fractional order fuzzy PID controller: Design, performance evaluation, and its optimal time domain tuning. *ISA Trans* 68: 251-75.
20. Al Gizi AJH, Mustafa MW, Al-geelani NA, Alsaedi MA (2015) Sugeno fuzzy PID tuning, by genetic-neutral for AVR in electrical power generation. *Appl Soft Comput* 28: 226-36.
21. Aguila-Camacho N, Duarte-Mermoud MA (2013) Fractional adaptive control for an automatic voltage regulator. *ISA Trans* 52: 807-15.
22. Pan I, Das S, Gupta A (2011) Tuning of an optimal fuzzy PID controller with stochastic algorithms for networked control systems with random time delay. *ISA Trans* 50: 28-36.
23. Batmani Y, Golpîra H (2019) Automatic voltage regulator design using a modified adaptive optimal approach. *Int J Electr Power Energy Syst* 104: 349-57.
24. Al Gizi A, Mustafa MW, Al Zaidi K, Al-Zaidi M (2015) Integrated PLC-fuzzy PID Simulink implemented AVR system. *Int J Electr Power Energy Syst*.
25. Shayeghi H, Younesi A, Hashemi Y (2015) Optimal design of a robust discrete parallel FP + FI + FD controller for the Automatic Voltage Regulator system. *Int J Electr Power Energy Syst* 67: 66-75.
26. Pan I, Das S (2012) Chaotic multi-objective optimization based design of fractional order PI λ D μ controller in AVR system. *Int J Electr Power Energy Syst* 43: 393-407.

27. Modabbernia M, Alizadeh B, Sahab A (2020) Mirhosseini Moghaddam M. Designing the Robust Fuzzy PI and Fuzzy Type-2 PI Controllers by Metaheuristic Optimizing Algorithms for AVR System. *IETE J Res* 1–15.
28. Chatterjee S, Mukherjee V (2016) PID controller for automatic voltage regulator using teaching–learning based optimization technique. *Int J Electr Power Energy Syst* 77: 418–29.
29. Nahas N, Abouheaf M, Sharaf A, Gueaieb W (2019) A Self-Adjusting Adaptive AVR-LFC Scheme for Synchronous Generators. *IEEE Trans Power Syst* 34: 5073–5.
30. Mukherjee V, Ghoshal SP (2007) Intelligent particle swarm optimized fuzzy PID controller for AVR system. *Electr Power Syst Res* 77: 1689–98.
31. Kim DH (2011) Hybrid GA–BF based intelligent PID controller tuning for AVR system. *Appl Soft Comput* 11: 11–22.
32. Micev M, Čalasan M, Ali ZM, Hasanien HM, Abdel Aleem SHE (2020) Optimal design of automatic voltage regulation controller using hybrid simulated annealing – Manta ray foraging optimization algorithm. *Ain Shams Eng J*.
33. Jumani TA, Mustafa MW, Hussain Z, Md. Rasid M, Saeed MS, Memon MM, et al. (2020) Jaya optimization algorithm for transient response and stability enhancement of a fractional-order PID based automatic voltage regulator system. *Alexandria Eng J* 59: 2429–40.
34. Sikander A, Thakur P, Bansal RC, Rajasekar S (2018) A novel technique to design cuckoo search based FOPID controller for AVR in power systems. *Comput Electr Eng* 70: 261–74.
35. Çelik E, Durgut R (2018) Performance enhancement of automatic voltage regulator by modified cost function and symbiotic organisms search algorithm. *Eng Sci Technol an Int J* 21: 1104–11.
36. Mokeddem D, Mirjalili S (2020) Improved Whale Optimization Algorithm applied to design PID plus second-order derivative controller for automatic voltage regulator system. *J Chinese Inst Eng* 43: 541–52.
37. Kose E (2020) Optimal Control of AVR System With Tree Seed Algorithm-Based PID Controller. *IEEE Access* 8: 89457–67.
38. Sahib MA (2015) A novel optimal PID plus second order derivative controller for AVR system. *Eng Sci Technol an Int J* 18: 194–206.
39. Niknam T, Azizipanah-Abarghooee R, Rasoul Narimani M (2012) A new multi objective optimization approach based on TLBO for location of automatic voltage regulators in distribution systems. *Eng Appl Artif Intell* 25: 1577–88.
40. Bernard MZ, Mohamed TH, Mitani Y, Qudaih YS (2013) CDM application on power system as a load frequency controller. 2013 IEEE Electr. Power Energy Conf., IEEE; 1–5.
41. Bernard MZ, Mohamed TH, Qudaih YS, Mitani Y (2014) Decentralized load frequency control in an interconnected power system using Coefficient Diagram Method. *Int J Electr Power Energy Syst* 63: 165–72.
42. Heshmati M, Noroozian R, Jalilzadeh S, Shayeghi H (2020) Optimal design of CDM controller to frequency control of a realistic power system equipped with storage devices using grasshopper optimization algorithm. *ISA Trans* 97: 202–15.
43. Mohamed TH, Shabib G, Ali H (2016) Distributed load frequency control in an interconnected power system using ecological technique and coefficient diagram method. *Int J Electr Power Energy Syst* 82: 496–507.
44. Ali R, Mohamed TH, Qudaih YS, Mitani Y (2014) A new load frequency control approach in an isolated small power systems using coefficient diagram method. *Int J Electr Power Energy Syst* 56:110-6.
45. Wolpert DH, Macready WG (1997) No free lunch theorems for optimization. *IEEE Trans Evol Comput* 1: 67-82.
46. Manabe S (1998) Coefficient Diagram Method. *IFAC Proc Vol* 31: 211-22.
47. Manabe S (2003) Importance of coefficient diagram in polynomial method. 42nd IEEE Int. Conf. Decis. Control (IEEE Cat. No.03CH37475), IEEE; n.d., p. 3489-94.
48. Manabe S (2005) Case studies of coefficient diagram method–practical polynomial design approaches. *IFAC Proc Vol* 38: 904-9.
49. Ghasemi M, Davoudkhani IF, Akbari E, Rahimnejad A, Ghavidel S, Li L (2020) A novel and effective optimization algorithm for global optimization and its engineering applications: Turbulent Flow of Water-based Optimization (TFWO). *Eng Appl Artif Intell* 92.

Submit your manuscript to a JScholar journal and benefit from:

- ¶ Convenient online submission
- ¶ Rigorous peer review
- ¶ Immediate publication on acceptance
- ¶ Open access: articles freely available online
- ¶ High visibility within the field
- ¶ Better discount for your subsequent articles

Submit your manuscript at
<http://www.jscholaronline.org/submit-manuscript.php>